Clean Energy Science and Technology 2025, 3(1), 334.
https://doi.org/10.18686/cest334

Article

Optimal control method for flexible loads in thermally activated buildings

Xiaochen Yang[1*], Ruizhi Wang[1], Zhenya Zhang[2], Ping Wang[2], Dingzhou Liu[1], Yixuan Jiang[1]

[1] Tianjin Key Laboratory of Built Environment and Energy Application, School of Environmental Science & Engineering, Tianjin University, Tianjin 300072, China
[2] Anhui Province Key Laboratory of Intelligent Building & Building Energy Saving, Anhui Jianzhu University, Hefei 230601, China
*** Corresponding author:** Xiaochen Yang, xiaochen.yang@tju.edu.cn

CITATION

Yang X, Wang R, Zhang Z, et al. Optimal control method for flexible loads in thermally activated buildings. Clean Energy Science and Technology. 2025; 3(1): 334. https://doi.org/10.18686/cest334

ARTICLE INFO

Received: 30 August 2024
Accepted: 3 December 2024
Available online: 21 January 2025

Abstract: As the penetration of renewable energy in the energy system continues to rise, the intermittency and stochasticity of energy supply have become increasingly significant, posing challenges to the dynamic coordination between energy supply and demand. Building thermal mass, with its inherent heat capacity, offers substantial energy storage potential, presenting a cost-effective alternative to traditional active energy storage methods. The activation and precise control of flexible energy from the building's thermal mass, has become a critical area of research. In this paper, based on a case floor-type thermally activated building system (TABS), the methods and constraints of simulating the energy flexibility potential on the demand side of the building were analyzed. By developing model predictive control (MPC) strategies, including white-box MPC, grey-box MPC, and black-box MPC, this study compared and assessed the control performance in terms of room temperature, accumulated energy cost, and the utilization efficiency of energy flexibility. Compared with the traditional rule-based control method, the MPCs showed better performance in room-temperature control, operation economics, and efficiency of flexible-load utilization, effectively saving energy costs by up to 20% and improving flexibility utilization by nearly 40%. Moreover, based on the performance comparison of the MPCs, white-box MPC performed optimally in terms of room-temperature control, while grey-box MPC was more effective in reducing energy costs and improving energy flexibility. The findings of this paper can provide theoretical insight for the efficient utilization of energy flexibility from building thermal mass and the selection of control methods.

Keywords: TABS; building energy flexibility; model predictive control; thermal inertia; multi-objective optimization

1. Introduction

At present, huge carbon dioxide emissions have caused serious energy and climate problems. To cope with the situation, countries have put forward carbon emission reduction measures. China put forward a dual-carbon target in 2020 and has been actively implementing energy upgrading and transformation in various industries. The building industry is one of the major areas of energy consumption and carbon dioxide emissions in China. In 2018 alone, the total energy consumption of buildings in China was 2.147 billion tons of standard coal equivalent, accounting for 46.5% of the country's total energy consumption. And carbon emissions from the building sector account for more than 50% of China's total carbon emissions [1]. Therefore, improving the energy efficiency of buildings and the penetration rate of renewable energy in the building sector is an effective way to achieve carbon neutral goal. In recent years, the production of renewable energy has been increasing, but due to its strong randomness, volatility, and intermittency, the mismatch between supply

and demand has resulted in serious energy waste. Utilizing the energy flexibility generated by the building's own thermal mass allows for an effective demand response, which is more economical and has a potentially larger scale than that of active energy storage. Energy flexibility in buildings is defined in IEA EBC Annex 67 [2] as "the ability to manage demand and production according to local climatic conditions, user needs, and energy network requirements." The concept of energy flexibility originated in the context of power systems, and its application to thermal systems is a more recent development. The fundamental idea remains the same: thermal loads, like electrical loads, can be shifted or regulated in real time, provided that human thermal comfort is maintained, despite the slower response times inherent to thermal system compared to power system. The effective utilization of flexible building energy can significantly mitigate the imbalance between supply and demand, thereby facilitating load shifting, reducing peak demand, and addressing the intermittent nature of renewable energy sources. Specifically, excess heat can be "stored" during periods of low demand and "released" during peak demand, thus not only alleviating peak load pressures but also meeting users' heating needs. Buildings hold substantial untapped potential for flexible thermal load adjustment; however, current demand-side management strategies face several challenges, including a lack of market mechanisms, policies, and technological advancements. As a result, the potential for establishing stable thermal loads and improving coordination within heat networks remains largely underutilized, limiting the broader role of thermal systems in integrated energy management. Therefore, investigating optimal methods for regulating demand-side heat flexibility is of great importance.

Thermally activated building system (TABS) embeds energy-supply tubes directly in building envelope, so to provide significant flexible load potential and lower heat loss and CO_2 emissions compared to the radiant-surface heating systems [3]. TABS implements load shifting, as well as peak shaving, by storing or releasing heat from the envelope through the adjustment of indoor temperature within the temperature range of thermal comfort. In addition, due to the large heat transfer area, the source temperature for cooling/heating can be very close to indoor set point temperature, making it more suitable for low-temperature heating (source temperature of 22–28 °C) or high-temperature cooling. As irreversible energy losses caused by the temperature difference during heat transfer are much reduced, the system has high efficiency and provides more opportunities for renewable energy and low-grade waste heat as the heat source (such as shallow geothermal energy, solar energy, etc.), further realizing building energy efficiency and the decarbonization of energy use. The current control for TABS can be generally categorized into on/off control, pulse-width control, regular control, and gain-adjustable control [3]. Traditional control methods, with their simple logic, can save building energy consumption and satisfy comfort needs to a certain extent [4–7]. However, there is usually a large time lag in the pipe-embedded energy supply system's response, which can be up to several hours depending on the depth of the tubes and the floor's heat capacity. Conventional on/off and proportional-integral (PI) control methods lack the ability to compensate for the thermal lag and fail to respond in a timely manner to sudden load changes in the indoor space [8,9]. If the thermal storage potential of the thermal mass of the envelope can be

fully utilized through advanced control methods, the peak demand-side load can be reduced by 26%–61% [10], while 44% energy savings can be achieved [4]. Model predictive control (MPC), which is based on a predictive and optimized control framework, can effectively address the effects of the thermal inertia of the pipe-embedded energy supply system and minimize the effects of uncertain heat disturbance on the control accuracy. Moreover, the control sequences can be optimized according to specific objectives. According to previous studies, compared with traditional control methods, the use of MPC for HVAC systems can save energy consumption by up to 40–50% [11] and operating costs by up to 51% [12]. Generally, based on different forms of building system's models, model predictive control can be divided into white-box, grey-box, and black-box MPCs.

Currently, research on flexible energy use in buildings mostly focuses on control strategies with active demand response, with relatively few studies exploring passive flexible-load regulation utilizing a building's intrinsic thermal mass. This type of regulation is affected by the thermal inertia of building envelope, which is difficult to be effectively addressed by traditional control methods. MPC, on the other hand, is an advanced optimization control method and can effectively deal with overshooting problems in the building's thermal system with large thermal inertia. However, the application of MPC in the energy flexibility regulation of building thermal mass has not been sufficiently studied. In addition, most of the studies on control strategies focus on specific cases using a single control method, and there is a lack of side-by-side comparison and systematic analysis of the performance of different control methods. In this paper, the activation and enhancing methods of flexible energy from building thermal mass are described. Due to the large energy flexibility potential, an experimental room with floor-type TABS is applied as reference. With the objectives of the indoor-temperature control accuracy, energy cost reduction, and efficiency of energy flexibility utilization, the study compared the performances of white-box, grey-box, black-box MPCs, as well as traditional control on the case TABS supplied by heat pump. The conclusions of this paper can provide theoretical insight and methodological support for the active utilization of flexible loads on the demand side of buildings, as well as for the efficient synergy between the supply and demand sides of renewable-based energy system.

2. Materials and methods

2.1. Description of the case TABS system

The case TABS system is located inside a climate chamber in Tianjin of Northern China. The test rig was established for the investigation of the TABS thermal behavior as well as the performance of the combined control strategy. An environmental chamber equipped with a precision air conditioning system is installed to provide required outdoor climate condition over temperature and humidity. The system enables precise regulation of the internal temperature within the range of 5 ℃ to 40 ℃, maintaining a fluctuation margin of ±1 ℃. The humidity control is within a range of 10% to 90% relative humidity (RH). With a maximum airflow capacity of 2000 m^3/h, the system is designed to meet the environmental requirements under diverse

operational conditions, including both summer and winter scenarios. **Figure 1a** shows the exterior appearance of the test rig. The dimension of the room is 2000 mm × 2000 mm × 1800 mm. The building envelope is designed meeting the low-energy building code of the local city. A window with the size of 600 mm × 600 mm is located on the south wall, so to include the impact of the solar radiation. This paper focused on winter heating conditions, and in order to ensure the universality of the results, the weather data of the coldest two weeks of a typical meteorological year (TMY), which were from February 1 to February 14, were selected for simulation. **Figure 2** shows the TMY outdoor temperature variation during the test period in Tianjin. The meteorological data were obtained from the EnergyPlus website [13].

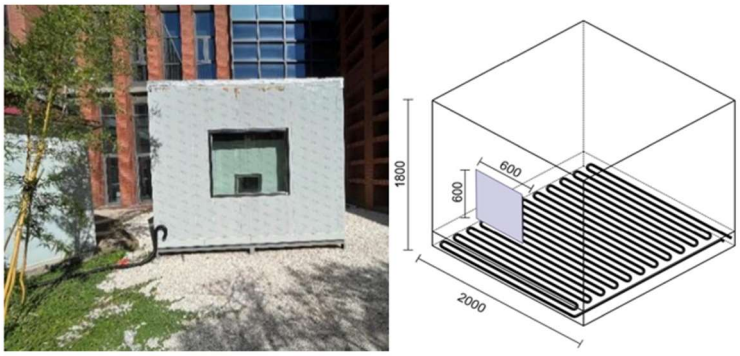

Figure 1. (a) The test rig that consists of the case room and the climate chamber; **(b)** layout of the case room with floor-type TABS.

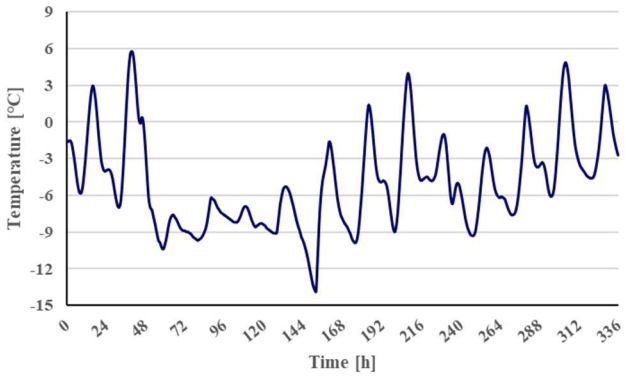

Figure 2. Outdoor temperature of typical meteorological year of the case building from 1st February to 14th February.

The indoor energy supply for the case study building is from the floor-type TABS, and the installation position of the embedded pipes and the arrangement of each material layer are shown in **Figure 3**, where the energy supply pipes are laid directly in the core layer made by concrete. The heat source of the test rig is an air-source heat pump, which can adjust the temperature of the primary-side water supply on demand. The heat pump has a rated input power of 1.37 kW, a maximum power of 1.644 kW, and a rated flow rate of 110 L/h. The heat pump is able to provide both heating and cooling for the test TABS. Under cooling conditions, the heat pump can provide an outlet water temperature ranging from 5 ℃ to 25 ℃, while under heating

conditions, it can supply water at temperatures up to 55 ℃, which meets the requirements for indoor heating and cooling purposes of radiant system. Moreover, a storage tank is installed between the heat pump and the TABS. The water tank not only serves as a reservoir for chilled or heated water but also acts as a buffer to balance the system's heating or cooling demands, thereby preventing significant temperature fluctuations that could affect the system operation. A temperature sensor is installed inside the tank to monitor the water temperature in real time and transmit the data to the heat pump controller. The controller can automatically adjust the heat output of the heat pump accordingly.

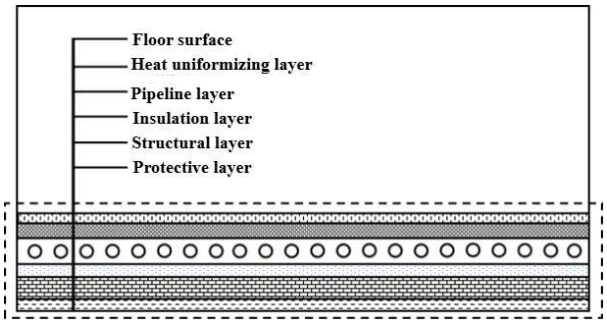

Figure 3. Composition of floor-type TABS.

2.2. Rule-based control method for the case TABS

The regulation of flexible loads in a TABS mainly relies on changing the set point of indoor temperature. The rule-based control (RBC) method, therefore, sets fixed indoor-temperature control values for different periods based on the consideration of the indoor thermal comfort standard, occupancy, and time-sharing tariffs of local policies. In this study, the range of the temperature for indoor thermal comfort was determined from the Design Code for Heating, Ventilation and Air Conditioning of Civil Buildings GB 50736-2012 standard, which establishes that in winter, the indoor heating temperature in severe-climate and cold regions should be designed at between 18 ℃–24 ℃, while the design indoor temperature for the radiant heating system should be 2 ℃ lower [14]. As the heat pump is the main heat source, the electricity price plays important role in the overall energy cost. The tiered electricity pricing at the local region is divided into the following periods: the trough period of 23:00–7:00, the flat periods of 7:00–8:00 and 11:00–18:00, and the peak periods of 8:00–11:00 and 18:00–23:00, as shown in **Table 1.**

Table 1. Local tiered electricity pricing.

Period	Electricity price type
00:00–07:00	Trough period
07:00–08:00	Flat period
08:00–11:00	Peak period
11:00–18:00	Flat period
18:00–23:00	Peak period
23:00–24:00	Trough period

In summary, the rule-based control strategy for the building heat supply is divided into the following periods. Between 0:00–8:00, when the price of electricity is relatively lower, which is during the trough and flat periods, the heat pump's is operated to maintain the indoor temperature at 22 ℃. Between 8:00–11:00, when the electricity price is in the peak period, and as the residents are assumed to go to work, the temperature is maintained at lower boundary of the thermal comfort temperature range, which is 18 ℃ at the lowest. At 11:00–18:00, when the electricity price is in the flat period, the heat pump controller is turned on to store more heat in advance, thereby reducing the peak pressure during the peak period right after. The implementation was done in advance to preheat and maintain the indoor temperature at the upper limit of the indoor thermal comfort temperature of 24 ℃ in order to reserve energy for peak-period use. From 18:00–23:00, it is sufficient to maintain the indoor temperature at 20 ℃, as the electricity tariff is at its peak. Between 23:00 and 24:00, when the electricity price is low, the heat pump is switched on to maintain the indoor temperature at 22 ℃. As the residents' thermal comfort is the priority, the heat pump is supposed to be switched on whenever the indoor temperature falls below the lower limit of the thermal comfort temperature, so to avoid any discomfort for the occupants.

2.3. MPC methods for the case TABS

MPC determines the current control action by using the mathematical model of a system to predict and optimize the future parameter status, which mainly includes a system prediction model, optimization objectives, and constraints. Compared with RBC, model predictive control has higher flexibility and adaptability. Therefore, this study established white-box MPC, grey-box MPC, and black-box MPC for the thermal system of the case study building in order to compare the operation effects of different control methods. Considering energy expenditure and the effect of indoor-temperature control, the target equations of model predictive control in this study are as follows:

$$J = \min_{u_1, u_2 \cdots u_k} \sum_{t=1}^{N-1} (r(q_{max}/COP_k) u_k p_{elec.k}) + q(T_k - T_{set.k})^2 \quad (1)$$

where N is the prediction time domain, which was set to 12 h considering the thermal behavior of the TABS; q_{max} is the maximal power of the heating pump; $p_{elec,k}$ is the price of electricity to drive the heat pump at moment k; COP_k is the COP of the heat pump at moment k; r and q are weight values, which were set to 50 and 1 concerning the different scale of temperature and power; u_k is the control input at time k; T_k is the indoor temperature at time k; and $T_{set,k}$ is the set value of the indoor temperature at time k.

2.3.1. White-box model predictive control

White-box MPC (W-MPC) is based on detailed physical models of case studies. The building physical model used in this paper was based on the Modelica modeling language. The model's structure and setup are similar to those of the RBC model, but the control of the input variable (heat supply of the case study) for W-MPC depends on the optimization result of the MPC objective function. A general optimization tool—Genopt is applied to obtain the optimal control sequence and Particle Swarm

Optimization (PSO) is used to solve the objective function with respect to thermal comfort requirements and the limitations of equipment's heat production. The computed optimal control sequence is fed to the controller module of the W-MPC. The MPC controller module receives hourly indoor temperature data from local sensors and conducts rolling optimization. The flowchart of the white-box MPC is shown in **Figure 4**.

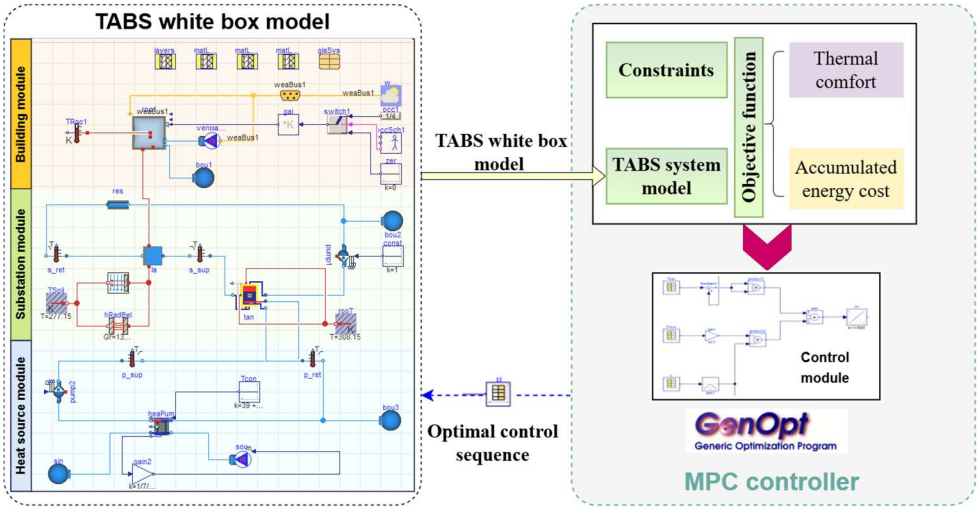

Figure 4. Flowchart of white-box MPC.

2.3.2. Grey-box model predictive control

Grey-box MPC (G-MPC) utilizes RC analogy for the physical model establishment, so to describe the thermal dynamics of a building [15]. Compared to the white-box model, the required physical information of grey-box model is much simplified. According to the heat transfer process of the case study building, the logic of the RC model of the case study is shown in **Figure 5**.

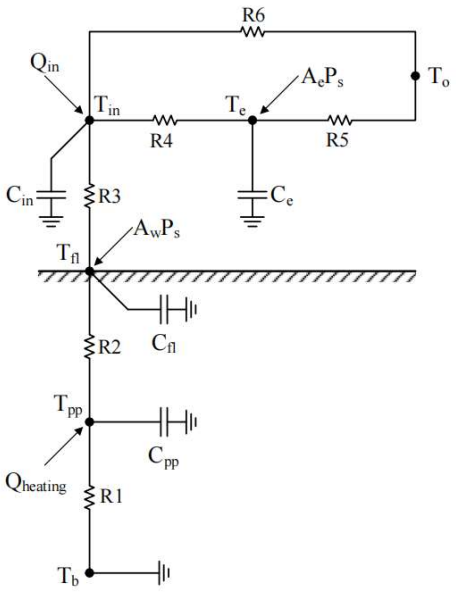

Figure 5. RC model of case study.

The heat balance equations of the case study are as follows:

$$C_{in}\frac{dT_{in}}{d\tau}=\frac{T_0-T_{in}}{R_6}+\frac{T_e-T_{in}}{R_4}+\frac{T_{fl}-T_{in}}{R_3}+Q_{in} \tag{2}$$

$$C_{fl}\frac{dT_{fl}}{d\tau}=\frac{T_{in}-T_{fl}}{R_3}+\frac{T_{pp}-T_{fl}}{R_2}+A_wP_s \tag{3}$$

$$C_{pp}\frac{dT_{pp}}{d\tau}=\frac{T_{fl}-T_{pp}}{R_2}+\frac{T_b-T_{pp}}{R_1}+Q_{heating} \tag{4}$$

$$C_e\frac{dT_e}{d\tau}=\frac{T_{in}-T_e}{R_4}+\frac{T_0-T_e}{R_5}+A_eP_s \tag{5}$$

where:

T_{in}—Indoor temperature, in ℃

T_{fl}—Floor surface temperature, in ℃

T_{pp}—Temperature of fluid in the embedded pipe, in ℃

T_e—Temperature of the building envelope, in ℃

T_o—Outdoor air temperature, in ℃

T_b—Soil temperature, in ℃

C_{in}—Indoor heat capacity, in kJ/m^2·K

C_{fl}—Floor heat capacity, in kJ/m^2·K

C_{pp}—Heat capacity of the heat carrier medium, in kJ/m^2·K

C_e—Heat capacity of the building envelope, in kJ/m^2·K

Q_{in}—Indoor thermal disturbance (lighting, people, facilities, etc.) in W

$Q_{heating}$—Heating system heat input, in W

P_s—Heat gain from solar radiation, in W/m^2

A_w—Area of transparent envelope for solar radiation directly entering the indoor environment, in m^2

A_e—Area of opaque envelope with solar radiation, in m^2

R_1—Thermal resistance of heat transfer between the embedded pipe and the soil, in m^2·K/W

R_2—Thermal resistance of heat transfer between the embedded pipe and the floor, in m^2·K/W

R_3—Thermal resistance between the floor and the indoor environment, in m^2·K/W

R_4—Thermal resistance between the indoor environment and the inner surface of the enclosure structure, in m^2·K/W

R_5—Thermal resistance between the outdoor environment and the outer surface of the enclosure structure, in m^2·K/W

R_6—Radiative heat transfer thermal resistance between the indoor environment and the outdoor environment, in m^2·K/W

Before starting model prediction, unknown model parameters should be determined based on parameter identification. In this study, unknown parameters were estimated using CTSM-R [16] using the data during the two-week test period. The objective function was solved using the YALMIP toolbox [17] and the Gurobi solver [18]. The flowchart of the grey-box MPC is shown in **Figure 6.**

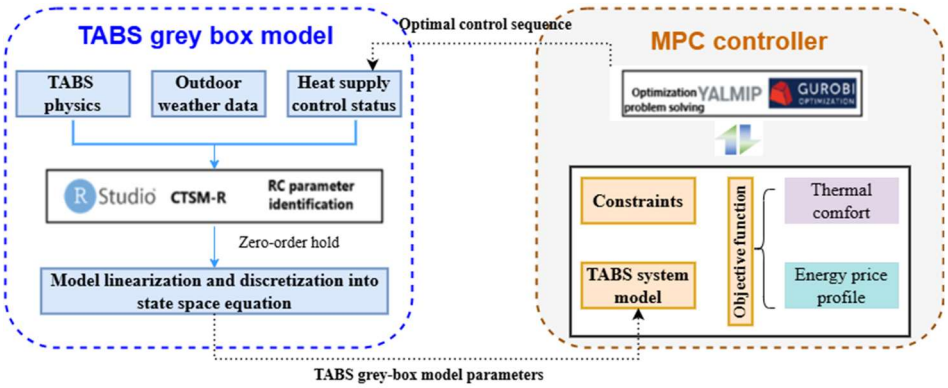

Figure 6. Flowchart of grey-box MPC.

2.3.3. Black-box model predictive control

Black-box MPC (B-MPC) is generally established from historical data. The Long Short-Term Memory (LSTM) network method, a type of neural network, was used in this study to train the black-box MPC model. In this case, outdoor temperature, solar radiation, control sequences, indoor occupancy, and historical indoor temperature data were collected as historical data. For each time step t, all features from t-12 to t (excluding indoor temperature) and indoor temperatures from t-12 to t-1 were used as feature sets. These features were combined into an input vector containing multi-step time-series features. The indoor temperature at time step t was used as the target value. This process would generate a feature-target pair dataset. After data cleaning and normalization, the dataset was divided into training and testing sets for the model in a ratio of 80%: 20%. The prediction model was continuously improved by reducing the error between the state parameters and the setpoint. After the LSTM prediction model was obtained, the predicted indoor temperature data would be transferred from black-box MPC to the controller via Python, and the Genetic Algorithm was used to solve the objective function, so as to obtain the optimal control sequence for the regulation of the heat pump's heat production. The optimal control sequence then was sent to the system model for the heat input regulation. The flowchart of the black-box MPC is shown in **Figure 7**.

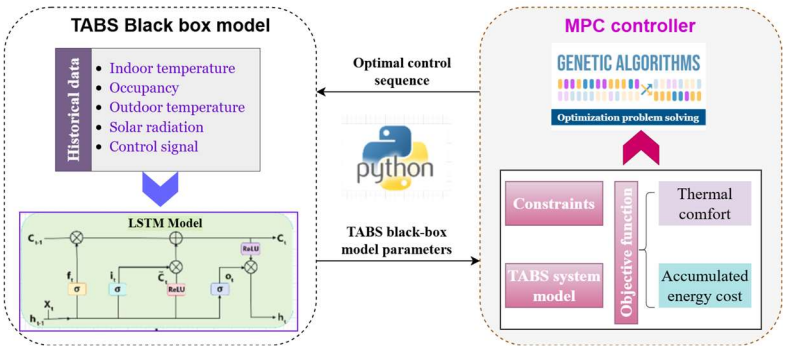

Figure 7. Flowchart of black-box MPC.

2.4. Performance evaluation indicators

In order to evaluate the operation performances of different control methods, different evaluation indexes were applied concerning the effect of room-temperature

control, accumulated energy cost, and efficiency of flexible energy utilization of the TABS. Equation (6) was used to calculate the system's violation of indoor temperature constraints under different control strategies, where $T_{simulate}(t)$ is the modeled indoor temperature.

$$T_{violate} = \sum_{t=1}^{N} |T_{simulate}(t) - \{T_{min}(t), T_{max}(t)\}| \quad (6)$$

Equation (7) was used to calculate the energy spent by the system under different control methods, where $P(t)$ is the power rate of the heat pump and $p_{elec}(t)$ is the electricity price at time *t*.

$$Cost = \sum_{t=1}^{N} P(t) p_{elec}(t) \quad (7)$$

Equation (8) was used to evaluate the effectiveness of energy flexibility utilization. The flexibility factor (FF) value ranges from –1 to 1. The best case is when FF = 1, which indicates that energy consumption can be shifted to the low-price period. On the contrary, an FF value of 0 indicates that a building's thermal mass has limited ability to utilize flexible loads and cannot effectively shift thermal loads to periods of low energy prices. The most unfavorable case is when FF = –1, indicating that energy consumption occurs during high-price periods and the system lacks the ability to adjust its thermal loads.

$$FF = \frac{\int_{low\ price\ time} Q_{heating}(t)\,dt - \int_{high\ price\ time} Q_{heating}(t)\,dt}{\int_{low\ price\ time} Q_{heating}(t)\,dt + \int_{low\ price\ time} Q_{heating}(t)\,dt} \quad (8)$$

3. Results and discussion

3.1. Validation of the system models

As the system model plays important role in developing the control strategy with effective and robust performance, the accuracy of white-box, grey-box and black-box system models of the test room were checked first. The simulated indoor temperature was compared with the measurements for model validation. The results are shown in **Figure 8**.

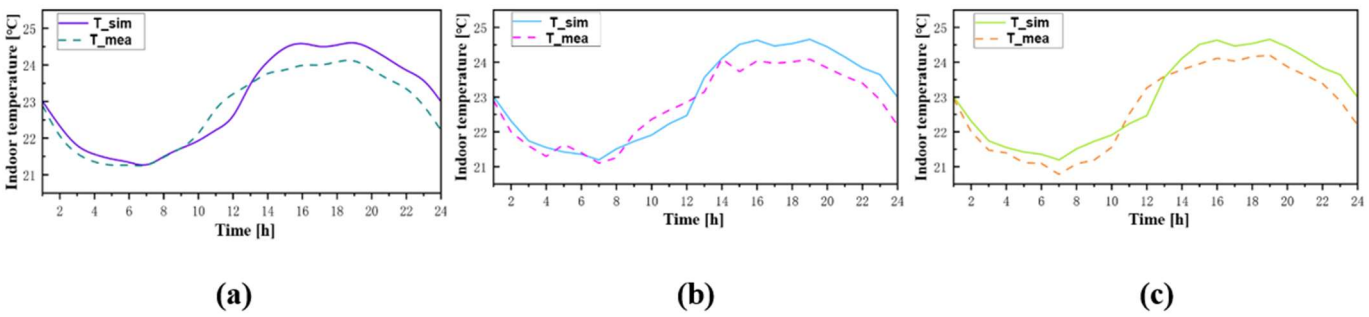

Figure 8. Deviation of the simulated indoor temperatures from **(a)** white-box model **(b)** grey-box model **(c)** black-box model and the measurements.

The results indicate that all three system models exhibit similar trends in variation and closely match the measured temperature values. The calculated root mean square errors (RMSE) are 0.447 ℃, 0.452 ℃, and 0.460 ℃ for the white-box, grey-box, and black-box models, respectively. These findings confirm that the developed simulation models effectively capture the system's dynamic thermal behavior, making them suitable for the establishment and investigation of model predictive control.

3.2. Performance of the indoor temperature control

The performances of the developed white-box, grey-box, and black-box MPC strategies and RBC were simulated for the test period. Regarding the temperature control, the indoor temperature under MPC shows less violation to the set point temperature range compared to RBC. The specific results are shown in **Figure 9**.

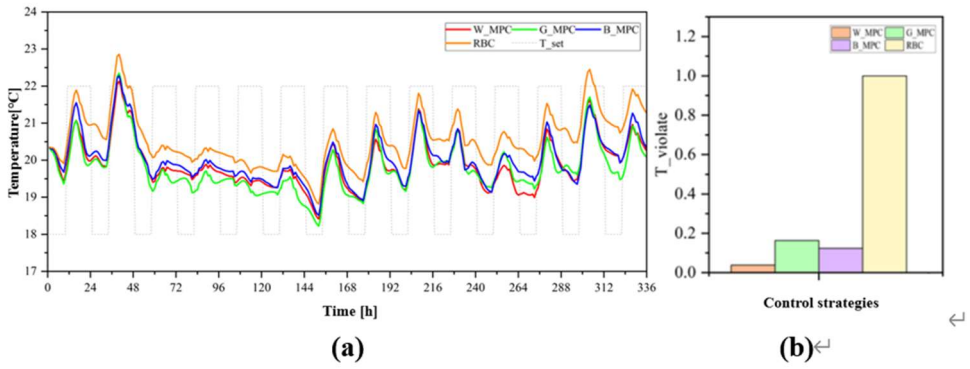

Figure 9. Effects of different control strategies' indoor temperature control. **(a)** indoor temperature variation under four control strategies; (**b)** the normalized violation of the indoor temperature constraint under four control strategies.

From **Figure 9a**, it can be seen that the temperature profiles of the MPCs are lower and closer to each other compared to RBC, which indicates that RBC is less efficient in controlling the indoor temperature of a building with high thermal inertia and is prone to overheating problems. On the contrary, the MPC strategy takes into account economic factors to keep the indoor temperature in a comfortable range and close to the lower limit of indoor temperature constraints. Regarding the violation of indoor temperature constraints, it can be seen from **Figure 9b** that the indoor temperature violation of the three MPC strategies is significantly lower compared to RBC as the baseline case for the normalized temperature. A side-by-side comparison of the three MPC strategies reveals that the violation of indoor temperature constraints is the least for white-box MPC, which reduced temperature violations by 3–34% compared with those of grey-box MPC and black-box MPC, respectively.

3.2. Total energy cost under different control strategies

As shown in **Table 2**, the total amount of energy consumed by the RBC strategy was the most significant among all the control strategies. The MPCs, on the other hand, due to the incorporation of multi-objective optimization, regulated the indoor temperature within a more reasonable range, hence avoiding overheating and reducing the overall heat supply. **Figure 10** illustrates the normalised heating cost of the system

under different control strategies. Using the performance of RBC as the normalized baseline, it can be seen that all three MPC strategies significantly reduce the accumulated energy cost. Since the effect of dynamic energy prices was taken into account in the objective equation, the MPC strategies preferred to operate the heat pump during periods of low electricity prices and utilize the energy flexibility of the TABS when the electricity prices were high. Comparing the economics of the three MPCs, grey-box MPC and white-box MPC outperformed black-box MPC, with grey-box MPC performing slightly better than white-box MPC.

Table 2. Total energy consumption by different control methods.

	W-MPC	G-MPC	B-MPC	RBC
Total energy consumption (kWh)	95.23	95.63	95.59	115.07

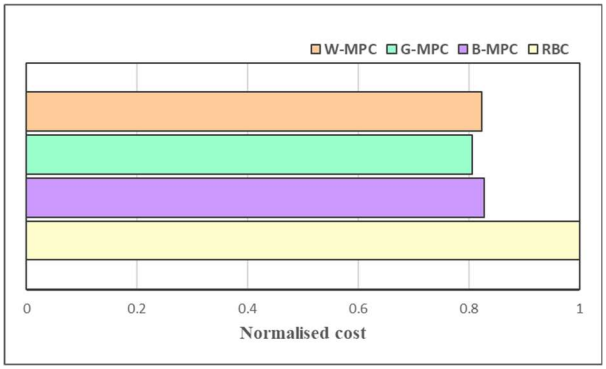

Figure 10. Normalized energy cost of different control methods.

3.3. Utilization efficiency of energy flexibility under different control strategies

The results of the efficiency of energy flexibility utilization of the system under the different control strategies are shown in **Figure 11**.

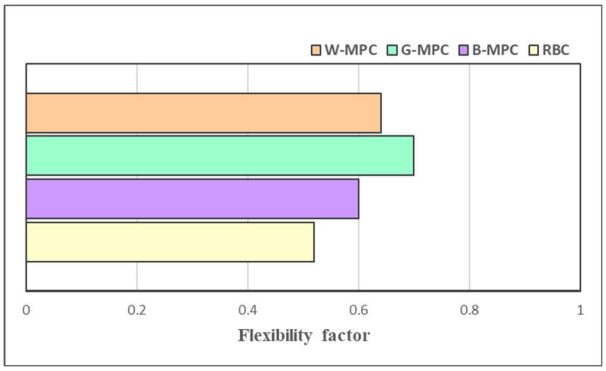

Figure 11. Normalised flexibility factor of different control methods.

The results show that all three MPC strategies had higher efficiency of energy flexibility utilization compared to that of RBC. Among the three MPC strategies, G-MPC shows the highest flexible-load utilization. Since the objective function of the MPCs considered energy cost and indoor comfort equally, it was difficult for the MPCs to completely shift the thermal loads to periods of low energy prices, and

therefore the flexibility utilization factors of the three MPC strategies were less than one.

4. Conclusions

This paper conducted research on the optimal control method of thermally activated building system, with the aim of activating and effectively utilizing the energy flexibility from the building thermal mass. A test rig with a floor-type TABS was applied as the reference case. White-box, grey-box, and black-box MPCs were established considering the indoor thermal comfort, accumulated energy cost, and the flexible energy utilization. Multidimensional evaluation of the developed control strategies was conducted, using the performance of RBC method as the baseline. The main conclusions are as follows:

(1) The accuracy of the white-box MPC model was higher overall, but it required a large number of model parameters as inputs. With sufficient historical data, the grey-box and black-box MPC models can accurately describe the dynamic thermal characteristics of the TABS.

(2) Compared with the traditional RBC method, the three MPC strategies showed better performance in room-temperature control, operation economics, and energy flexibility utilization. The prediction-based control strategies maintain more stable indoor temperature and effectively reduced the indoor temperature violations by up to 98%. By considering the dynamic price of energy and flexible-load utilization in the target equation, the MPCs saved the energy cost by up to 20% and improved flexibility utilization by nearly 40%.

(3) Among the three MPCs, white-box MPC showed the optimal performance in room-temperature control, while grey-box MPC was more effective in reducing energy costs and increasing energy flexibility utilization.

Author contributions: Conceptualization, XY; resources, XY; funding acquisition, XY; project management, XY; methodology, ZZ and PW; software, DL; validation, DL; formal analysis, DL; survey, RW; data organization, YJ. All authors have read and agreed to the published version of the manuscript.

Funding: This study was funded by the National Natural Science Foundation of China (Project No. 52208120), and the Opening Fund of Anhui Province Key Laboratory of Intelligent Building & Building Energy Saving, Anhui Jianzhu University (Project No. IBES2024KF07).

Conflict of interest: The authors declare no conflict of interest.

References

1. Fan L. Current status of carbon emissions in China's construction industry and the path to carbon neutrality through "solar energy storage, direct current and flexible power generation" (Chinese). Chongqing Architecture. 2021; 20(10): 23-25.
2. Jensen SØ, Marszal-Pomianowska A, Lollini R, et al. IEA EBC Annex 67 Energy Flexible Buildings. Energy and Buildings. 2017; 155: 25-34. doi: 10.1016/j.enbuild.2017.08.044
3. Hassan MA, Abdelaziz O. Best practices and recent advances in hydronic radiant cooling systems – Part II: Simulation, control, and integration. Energy and Buildings. 2020; 224: 110263. doi: 10.1016/j.enbuild.2020.110263

4. Li T, Merabtine A, Lachi M, et al. Experimental study on the thermal comfort in the room equipped with a radiant floor heating system exposed to direct solar radiation. Energy. 2021; 230: 120800. doi: 10.1016/j.energy.2021.120800
5. Guo J, Dong J, Wang H, et al. On-site measurement of the thermal performance of a novel ventilated thermal storage heating floor in a nearly zero energy building. Building and Environment. 2021; 201: 107993. doi: 10.1016/j.buildenv.2021.107993
6. Le Dréau J, Heiselberg P. Energy flexibility of residential buildings using short term heat storage in the thermal mass. Energy. 2016; 111: 991-1002. doi: 10.1016/j.energy.2016.05.076
7. Foteinaki K, Li R, Heller A, et al. Heating system energy flexibility of low-energy residential buildings. Energy and Buildings. 2018; 180: 95-108. doi: 10.1016/j.enbuild.2018.09.030
8. Chen T. Application of adaptive predictive control to a floor heating system with a large thermal lag. Energy and Buildings. 2002; 34(1): 45-51. doi: 10.1016/S0378-7788(01)00076-7
9. Rhee KN, Olesen BW, Kim KW. Ten questions about radiant heating and cooling systems. Building and Environment. 2017; 112: 367-381. doi: 10.1016/j.buildenv.2016.11.030
10. Kattan P, Ghali K, Al-Hindi M. Modeling of under-floor heating systems: A compromise between accuracy and complexity. HVAC&R Research. 2012; 18(3): 468-480. doi: 10.1080/10789669.2012.649881
11. Dussault JM, Sourbron M, Gosselin L. Reduced energy consumption and enhanced comfort with smart windows: Comparison between quasi-optimal, predictive and rule-based control strategies. Energy and Buildings. 2016; 127: 680-691. doi: 10.1016/j.enbuild.2016.06.024
12. Liu Y, Pan Y, Huang Z. Simulation study on air conditioning system operation optimization based on model predictive control (Chinese). In: Proceedings of the Shanghai Society of Refrigeration 2013 Annual Academic Conference; 18 December 2013; Shanghai, China. pp. 413-419.
13. EnergyPlus. Weather data. Available online: https://energyplus.net/weather (accessed on 25 July 2024).
14. GB50736-2012 Design code for heating ventilation and air conditioning of civil buildings. Available online: http://www.iwuchen.com/m/show.php?filename=1081 (accessed on 1 December 2024).
15. Drgoňa J, Arroyo J, Cupeiro Figueroa I, et al. All you need to know about model predictive control for buildings. Annual Reviews in Control. 2020; 50: 190-232. doi: 10.1016/j.arcontrol.2020.09.001
16. Juhl R, Møller JK, Madsen H. ctsmr - Continuous Time Stochastic Modeling in R. Available online: https://arxiv.org/abs/1606.00242 (accessed on 1 December 2024).
17. Lofberg J. YALMIP : A Toolbox for Modeling and Optimization in MATLAB. In: Proceedings of the 2004 IEEE International Conference on Robotics and Automation (IEEE Cat No04CH37508); 2-4 September 2004; Taipei, Taiwan. pp. 284-289. doi: 10.1109/cacsd.2004.1393890
18. Gurobi Optimization. Gurobi Optimizer Reference Manual. Available online: https://docs.gurobi.com/projects/optimizer/en/current/ (accessed on 1 December 2024).